Mutagenesis vol. 28 no. 3 pp. 357–366, 2013
Advance Access publication 28 February 2013
doi:10.1093/mutage/get009

Artemis is required to improve the accuracy of repair of double-strand breaks with 5′-blocked termini generated from non-DSB-clustered lesions

Svitlana Malyarchuk[1], Reneau Castore[1], Runhua Shi[2] and Lynn Harrison[1,*]

[1]Department of Molecular and Cellular Physiology, Louisiana Health Sciences Center, 1501 Kings Highway, Shreveport, LA 71130, USA and [2]Department of Medicine and Feist-Weiller Cancer Center, LSUHSC-S, Shreveport, LA, USA

*To whom correspondence should be addressed. Tel: +1-318-675-4213; Fax: +1-318-675-6005; Email: lclary@lsuhsc.edu

Received on July 23, 2012; revised on January 4, 2013; accepted on January 14, 2013

Clustered DNA lesions are defined as ≥2 damage events within 20 bp. Oxidised bases, abasic (AP) sites, single-strand breaks and double-strand breaks (DSBs) exist in radiation-induced clusters, and these lesions are more difficult to repair and can be more mutagenic than single lesions. Understanding clustered lesion repair is therefore important for the design of complementary treatments to enhance radiotherapy. Non-DSB-clustered lesions consisting of opposing AP sites can be converted to DSBs by base excision repair, and non-homologous end-joining (NHEJ) plays a role in repairing these DSBs. Artemis is an endonuclease that removes blocking groups from DSB termini during NHEJ. Hence, we hypothesised that Artemis plays a role in the processing of DSBs or complex DSBs generated from non-DSB-clustered lesions. We examined the repair of clusters containing two or three lesions in wild-type (WT) or Artemis-deficient (ART$^{-/-}$) mouse fibroblasts using a reporter plasmid. Each cluster contained two opposing tetrahydrofurans (an AP site analogue), which AP endonuclease can convert to a DSB with blocked 5′ termini. Loss of Artemis did not decrease plasmid survival, but did result in more mutagenic repair with plasmids containing larger deletions. This increase in deletions did not occur with ClaI-linearised plasmid. Since Mre11 has been implicated in deletional NHEJ, we used small interfering RNA to reduce Mre11 in WT and ART$^{-/-}$ cells, but decreasing Mre11 did not change the size of deletions in the repair products. This work implicates Artemis in limiting the deletions introduced during repair of 5′-blocked termini DSBs generated from non-DSB-clustered lesions. Decreasing repair accuracy without decreasing repair capacity could result in mutated cells surviving irradiation. Inhibiting Artemis in normal cells could promote carcinogenesis, while in tumour cells enhanced mutagenic repair following irradiation could promote tumour recurrence.

Introduction

Ionising radiation releases large amounts of energy and the average energy deposited in the medium per unit length of the radiation track is the linear energy transfer (LET) of the radiation. X-rays and gamma rays are low LET radiation, whereas alpha particles and heavy charged ions such as carbon (^{12}C) and iron (^{56}Fe) are high LET radiation and are more densely ionising. The critical target in the cell for ionising radiation is the DNA (1,2). Damage can result from the direct ionisation of the DNA as well as from hydroxyl radicals generated from the ionisation of water. Chemical alterations occur at guanine, thymine, adenine and cytosine, bases are released resulting in abasic (AP) sites, protein and DNA cross-links form and single-strand breaks (SSBs) and double-strand breaks (DSBs) are generated in the DNA (3,4). The termini of the breaks are frequently modified: 30% of 3′ termini contain a 3′ phosphoglycolate and 70% have a phosphate group attached (5,6). Strand breaks with 5′-blocked termini can also be generated following oxidation of the deoxyribose moiety (7): oxidation can directly generate strand breaks with a nucleoside 5′ aldehyde on the 5′ terminus or can produce oxidised AP sites that can be converted by a class II AP endonuclease to strand breaks with 5′-blocked termini (8,9).

Ionising radiation whether high or low LET can generate clusters of damage with ≥2 damages within 1–2 helical turns of the DNA (10,11). Since the yields of radiation-induced damage are in the order of base damage and AP sites > SSBs ≫ DSBs (12–14), clusters consisting of base damage, AP sites and SSBs occur more frequently than DSBs (11). These clusters are designated non-DSB clusters [for review, see ref. (15)]. DSBs can also be generated with nearby oxidative base damage and these are termed complex DSBs. Complex DSBs are predicted to be induced at a greater frequency (16) by high LET radiation. These DSBs are therefore a significant type of biological damage as high LET radiation is used to treat cancer (e.g. carbon ions) and is the relevant radiation for space exploration.

The base excision repair (BER) pathway is the predominant repair mechanism for base damage, AP sites and SSBs [for review, see ref. (17)]. Initiation of repair at base damage by BER produces a SSB repair intermediate and so non-DSB clusters with the lesions situated in opposing DNA strands can be converted to DSBs by BER. Work *in vitro* [for review, see ref. (18)] using pure enzymes and synthetic clustered lesions has demonstrated the production of DSBs from non-DSB-clustered lesions. However, non-DSB clusters of oxidised base damage are not readily converted to DSBs in cells (19,20). In fact in bacteria, closely opposed 8-oxo-7,8 dihydroguanine (8oxoG) residues enhance the mutation frequency of 8oxoG in the cluster (19,21), and the increase in mutation frequency is likely due to repair inhibition at the second 8oxoG after removal and introduction of a SSB at the first 8oxoG. This repair inhibition can be overcome in mammalian cells by over-expressing the 8oxoG DNA glycosylase: TK6 cells over-expressing Ogg1 have increased sensitivity to ionising radiation (22). Unlike base damage, opposing AP sites are readily converted to DSBs in prokaryotes and eukaryotes (23–26), and in mammalian cells, the major class II AP endonuclease has been implicated in this process (20,25). Non-DSB-clustered lesions consisting of opposing AP sites and nearby oxidative damage can also be converted to complex DSBs in mammalian cells (20).

DSBs and complex DSBs are potentially lethal lesions that are repaired by either homologous recombination or non-homologous end-joining [NHEJ; for review, see ref. (27)].

NHEJ is the predominant pathway in mammalian cells and is initiated by the binding of the Ku70/80 heterodimer at the termini of DSBs, which recruits the DNA-dependent protein kinase catalytic subunit (DNA-PKcs) to the damage site. The termini then undergo processing to remove blocking groups from the termini. In preparation for DNA ligation, nucleotides can be added or removed by DNA polymerases and/or nucleases, and repair is completed by XRCC4/DNA ligase IV/XLF.

Artemis and Mre11 are nucleases that are involved in the termini processing step of DSB repair, and there is evidence to suggest that Artemis is involved in modifying termini of complex DSBs (28). Artemis has 5′–3′ exonuclease activity specific for single-stranded DNA, but in the presence of DNA-PK, Artemis has endonuclease activity and is involved in the removal of 3′ phosphoglycolate termini and 5′ overhangs, in the shortening of 3′ overhangs at DSBs and in the opening of hairpin ends (29–31). Artemis-deficient (ART$^{-/-}$) cells are sensitive to ionising radiation, bleomycin and neocarzinostatin (32), and these defects can be complemented by expression of wild-type (WT) Artemis, but not an endonuclease-deficient mutant. ART$^{-/-}$ cells and the endonuclease mutant expressing cells are defective in repairing ~10–20% of DSBs, implicating the Artemis endonuclease activity in repair of a subset of breaks. These DSBs are generally repaired with slower kinetics (2–20 h) and have been suggested to be complex DSBs (33), DSBs with modified termini (32) or DSBs that are situated in heterochromatin (34,35). Mre11 has also been implicated in the repair of DSBs by NHEJ (36,37). Mre11 has endonuclease activity on single-stranded DNA, 3′–5′ exonuclease activity on double-stranded DNA and in combination with Rad50 and Nbs1 is essential for the generation of the long 3′ single-stranded DNA required for DSB repair by homologous recombination [for review, see ref. (38)]. Mre11 also plays a role in the post-DNA-incision steps of BER in yeast (39), and so Mre11 may be involved in termini processing in BER.

Previously, we used non-DSB clusters consisting of two opposing tetrahydrofuran (furan) lesions to demonstrate that this non-DSB cluster can be converted to a DSB in mouse cells by the major class II AP endonuclease, Apex1 (25). Apex1 cleaves at a furan on the 5′ side of the damage, generating a SSB in the DNA with a 3′ hydroxyl terminus that can be used by DNA polymerase β to insert a nucleotide, but with a 5′ terminus that is blocked. Repair, therefore, has to proceed by long patch BER as has been found for oxidised AP sites generated by ionising radiation (8,9). Cleavage at two opposing furans, therefore, results in a DSB with 5′-blocked termini that have to be removed prior to DNA end-joining, and our previous studies implicated both Ku-dependent and Ku-independent end-joining in the repair of these DSBs (25). We have also shown that two opposing furans with nearby 8oxoG can be converted to complex DSBs by Apex1 in mouse cells (20). To determine the involvement of Artemis in the completion of repair of the DSBs or complex DSBs generated from non-DSB clusters, we have now transfected a luciferase reporter plasmid containing either two opposing furans or two opposing furans with a nearby 8oxoG into WT or ART$^{-/-}$ mouse cells. We have examined cleavage of the non-DSB clusters, plasmid survival and the products of repair. We have also used small interfering RNA (siRNA) to reduce Mre11 expression in the WT and ART$^{-/-}$ cells and determined that Artemis, but not Mre11, plays a role in limiting the deletions during repair of the DSBs formed from two opposing furans. The situation of an 8oxoG near to the DSB generated from the furans did not alter the outcome of repair.

Materials and methods

Oligodeoxyribonucleotides

Oligodeoxyribonucleotides (oligonucleotides) were purchased from Operon Technologies Inc. (Alameda, CA). The sequences of the double-stranded oligonucleotides containing no damage or closely opposed tetrahydrofurans (furans, known as a d-spacer from Operon Technologies) and 8oxoG are shown in Table I. These oligonucleotides contained a 5′ phosphate and were purified using polyacrylamide gel electrophoresis. The presence of the damage was confirmed by labelling each oligonucleotide at the 5′ end with ^{32}P and performing *in vitro* assays as described in ref. (20) with endonuclease IV or Fpg.

Oligonucleotides that were used for polymerase chain reaction (PCR) analysis were not purified and did not contain 5′-phosphate termini. Two primer sets were used to amplify the luciferase region: Luc1 d(TGGATGGCTACATTCTG) and R d(TCATCGTCTTTCCGTGCT), Luc3 d(ATGTGGATTTCGAGTCGTCTT) and Luc5 d(GCCTGGTATCTTTATAG).

Plasmids

pCMV3′luc (40) encodes carbenicillin resistance in bacteria and expresses firefly luciferase from the cytomegalovirus promoter in mammalian cells. There are unique PacI and ClaI restriction sites in the 3′ end of the firefly luciferase coding region. pCMV3′luc inactive was generated by inserting a double-stranded oligonucleotide at the PacI site (25), which results in the expression of inactive firefly luciferase protein. pCMV3′luc inactive is digested with PacI and ClaI to generate the linear DNA that is used in the ligations with the double-stranded oligonucleotides shown in Table I. Insertion of the oligonucleotide sequences regenerates the pCMV3′luc sequence and expression of active firefly luciferase. Using pCMV3′luc inactive to generate the linear DNA eliminates potential background luciferase activity from the re-circularisation of partially digested plasmid in the ligation products. pACYC184 (New England Biolabs, Beverly, MA) is a low copy vector with a p15A origin of replication that encodes resistance to chloramphenicol (34 μg/ml). pRL-CMV (Promega, Madison, WI) expresses renilla luciferase in mammalian cells and encodes carbenicillin resistance.

Table I. The sequence of the insert between PacI and ClaI in pCMV3′luc

Name of lesion	Position of the F relative to the F on the NT strand (base pairs apart)	Position of the O relative to the F on the NT strand	Sequence
Undamaged	–	–	5′ TAAATACAAAGGATATCAGGTGGCCCCCGCTGAATTGGAAT 3′ (NT) 3′ TAATTTATGTTTCCTATAGTCCACCGGGGGCGACTTAACCTTAGC 5′ (T)
I	5	–	5′ TAAATACAAAGGATATCAGG**F**GGCCCCCGCTGAATTGGAAT 3′ (NT) 3′ TAATTTATGTTTCCTA**F**AGTCCACCGGGGGCGACTTAACCTTAGC 5′ (T)
II	5	5′	5′ TAAATACAAAGGATATCAG**OF**GGCCCCCGCTGAATTGGAAT 3′ (NT) 3′ TAATTTATGTTTCCTA**F**AGTCCACCGGGGGCGACTTAACCTTAGC 5′ (T)

F designates the position of a furan and **O** designates the position of an 8oxoG in a damage-containing oligonucleotide. Two oligonucleotides were annealed to form a clustered lesion. The NT strand is the non-transcribed strand and the T strand is the transcribed strand in pCMV3′luc.

Cell lines

Immortalised mouse fibroblast cell lines (41) that were WT or 'knocked-out' for the Artemis gene ($ART^{-/-}$) were kindly provided by Dr P. Jeggo (University of Sussex, East Sussex, UK), but they were originally generated in the laboratory of Dr Alt (Howard Hughes Medical Institute, Boston, MA, USA). Cells were maintained in Dulbecco's modified Eagle's medium containing 10% foetal bovine serum in a humidified atmosphere at 37°C in 10% CO_2.

Insertion of double-stranded oligonucleotides into pCMV3′luc

This was performed according to Malyarchuk *et al.* (25). Briefly, pCMV3′luc inactive was digested with PacI and ClaI and purified from an agarose gel following gel electrophoresis. Linear DNA was quantified using an Agilent 2100 Bioanalyzer (Agilent Technologies, Wilmington, DE). To generate double-stranded oligonucleotides (Table I), complementary oligonucleotides were mixed in equimolar amounts in 10 mM Tris–HCl (pH 8) and 50 mM NaCl and the reaction placed in water at >85°C. The annealing reactions were cooled to room temperature over a period of ~2.5 h.

To generate one sample of ligated product, three ligation reactions were performed and de-salted using the Qiaquick Nucleotide Removal kit (Qiagen Inc., Valencia, CA) before being pooled (final volume 90 µl). Each ligation reaction contained PacI–ClaI-digested pCMV3′luc inactive (~1.4 pmol or 5.5 µg), double-stranded oligonucleotide (7 pmol), 15 units of T4 DNA ligase (Promega Corporation, Madison, WI) and reaction buffer supplied by the manufacturer (0.5 mM adenosine triphosphate, 15 mM Tris–HCl pH 7.8, 5 mM $MgCl_2$, 5 mM dithiothreitol, 2.5% polyethylene glycol). Reactions were incubated overnight at 4°C. In order to have three different DNA samples for each insert, this procedure was performed in triplicate using different annealing reactions. A similar sample of DNA was also generated as a control from ligation reactions that did not contain oligonucleotide (control ligation).

Introduction of DNA into the mouse fibroblasts

To transfect DNA into the cells, we used the Nucleofector™ (AMAXA Biosystems, Gaithersburg, MD) and the MEF Nucleofector™ Kit 2, according to the manufacturer's instructions using program T-20. To test the ligated product for each insert or the control ligated product, 10 µl of DNA sample (~1.8 µg) and 10 ng of pRL-CMV or 100 ng of pACYC184 were co-transfected into 2×10^6 to 3×10^6 mouse fibroblast cells. pRL-CMV was used when cell-free extracts were prepared to measure luciferase activities, while pACYC184 was used for experiments where the DNA was re-isolated from the cells. At least five transfections were performed for each type of ligation to measure luciferase activity, and three different reactions for each type of ligation were transfected for plasmid survival experiments. ClaI-linearised pCMV3′luc was also transfected as a control for DNA with a DSB that did not require removal of 5′- or 3′-modified termini. pCMV3′luc was digested with ClaI, subjected to gel electrophoresis and purified from the gel. This procedure was repeated and the DNA quantified using an Agilent 2100 Bioanalyzer (Agilent Technologies, Wilmington, DE). ClaI-linearised pCMV3′luc (400 ng) was co-transfected with 100 ng pACYC184. The DNA was re-isolated from cells, and the DNA from two transfections was pooled to form one sample. Three samples of DNA per cell type were generated for plasmid survival experiments.

Measurement of firefly and renilla luciferase activities

Six hours following DNA transfection, cell-free extracts were prepared, and firefly and renilla luciferase assays were performed as described in Malyarchuk *et al.* (25). In each experiment, the ratio of firefly/renilla luciferase activity was calculated for each transfection, and an average ratio from three transfections of the undamaged sequence was determined and set at 100%. The activity ratio from each transfection in the experiment was then expressed as a percentage of this average ratio for the undamaged sequence. This was also calculated for the transfections of the undamaged sequence to allow us to determine the level of variation for the undamaged sample. At least six transfections were performed for each type of ligation and the results were used to calculate the average percentage of the activity ratio compared with the undamaged sequence and the standard error for each construct. The InStat3 program and the unpaired *t*-test with Welch correction was used to determine statistical differences between the results for the WT and $ART^{-/-}$ cells for the same type of construct. Transfection of the control ligation resulted in negligible firefly luciferase activity.

Down-regulation of mouse Mre11 using siRNA

siGENOME SMART pool against mouse Mre11 and siCONTROL RISC-free siRNA (negative control) were purchased from Dharmacon Inc. (Chicago, IL, USA). The target sequences for mouse MRE11A siRNA were GGAUGGCAAUCUCAACAUU, GCGAAGCAGUUCAAGAGUU, UAGAGUAGAAGACCUCGUA and UCGAGGAAUUAGUGAAGUA. One hundred picomoles (1.5 µg) of siRNA were transfected into the cells using the standard conditions described above. Three sets of transfections were performed at the same time: mock (no siRNA), negative control siRNA and a sample to decrease Mre11 expression (siRNA designed against Mre11). After 24 h, a sample of the transfected cells was used to prepare cell-free extracts. The remainder of the cells were then re-transfected with the pCMV3′luc ligation products as described above. The cell-free extracts were probed by western analysis to examine expression of Mre11 (mouse anti-Mre11 antibody, BD Biosciences, San Diego, CA, USA) and actin (anti-β-actin antibody, BD Biosciences, San Jose, CA, USA). Bound primary antibody was visualised using autoradiography following incubation with a secondary horseradish peroxidase antibody (Amersham, Piscataway, NJ, USA) and chemiluminescent substrate (ECL-plus substrate, Amersham, Piscataway, NJ, USA).

Plasmid survival assay and analysis of re-isolated DNA

Ligation reactions for each type of ligation or ClaI-linearised DNA were co-transfected with pACYC184 into WT and $ART^{-/-}$ cells, or cells that had been first transfected to down-regulate Mre11, as described above. The pACYC184 was added to the transfection to allow for normalisation of the transfection efficiency, the yield of the re-isolated DNA and the transformation efficiency into the bacteria. Two hours after transfection, the DNA was re-isolated from the cells as described in Malyarchuk *et al.* (25). A 2-h time point was chosen as in previous experiments we examined re-isolated DNA at 2 and 6 h and found that even by 6 h DNA degradation occurred from plasmid that contained only one DNA lesion (20). Each re-isolated DNA sample was transformed in duplicate into Max efficiency DH10B™ chemically competent cells (Invitrogen Corporation, Carlsbad, CA) and the culture grown on solid medium containing 100 µg/ml of carbenicillin or 34 µg/ml chloramphenicol. After overnight growth, a ratio of the carbenicillin-resistant ($Carb^R$) colonies/chloramphenicol-resistant (Cm^R) colonies was calculated for each transformation. The ratios were used to calculate the percentage of plasmid survival for each type of ligation compared with the undamaged sequence. The InStat3 program and the unpaired *t*-test with Welch correction or the Mann–Whitney test was used to determine statistical differences between the plasmid survival results of the same type of ligation in the different types of cells.

To determine the presence of deletions in the repair products in the colonies from the plasmid survival experiments, PCR was performed on the bacteria. To obtain a good sample size and a representative sample, colonies were randomly selected from the plasmid survival colonies from all three ligations and pooled for a type of substrate and cell line. $Carb^R$ colonies were re-grown and a small amount of the bacteria used in a PCR reaction. PCR was performed as previously described (25) using primer sets Luc1 and R, and Luc3 and Luc5. A small percentage of colonies examined using the Luc1 and R primer set generated products at the size of pCMV3′luc inactive (292 bp versus 236 bp for pCMV3′luc). These were eliminated from the analysis. Two types of statistical analyses were performed using the SAS/STAT Software 9.2 of SAS system for Windows (SAS Institute Inc., Cary, NC, USA) comparing the repair products for each DNA substrate between the WT and $ART^{-/-}$ cells or between the mock/siControl-transfected cells and the siMre11-transfected cells. The first statistical test was Fisher's exact test, which examined whether there was an increase or decrease in the proportion of colonies containing deletions between the cell types, or types of transfected cells. For this test, two groups of repair products were considered: those without deletions and those with deletions. A two-sided P value <0.05 was considered significant. A second analysis was performed with two different tests to consider whether the size of deletions in the colonies for a particular sample differed between the cell types, or types of transfected cells. From the product sizes of the PCR reactions, the colonies for each repair substrate were assigned to groups by size of deletion: 0, <100, 100–1000 and >1000 bp. This second analysis considers all the size groups together. For each repair substrate, the number of colonies in each group for either WT and $ART^{-/-}$ cells, for mock- and siMre11-transfected WT cells, or siControl- and siMre11-transfected $ART^{-/-}$ cells were compared. The chi-square test was first performed to determine whether the proportion of colonies with the different deletion sizes differed for a particular substrate between cell types or types of transfected cells. The Cochran Armitage Trend Test was then performed as a follow-up test to determine whether there was a trend in the proportion of colonies to contain greater or smaller deletion sizes for a particular cell type, or type of transfected cell. A two-sided P value <0.05 was considered significant in both of these tests.

Results

Loss of Artemis did not alter cleavage at the non-DSB-clustered lesions

We previously determined that two opposing furans, or a more complex lesion with two opposing furans and a nearby 8oxoG

(see Table I for the sequences), could be cleaved by Apex1 in mouse cells to generate DSBs (20,25). To examine the importance of Artemis in the repair of these non-DSB clusters, plasmid was transfected into ART$^{-/-}$ cells and the corresponding WT mouse cell line. Double-stranded oligonucleotides that were undamaged or that contained the non-DSB clusters were ligated into the coding region of firefly luciferase in pCMV3′luc. The ligations were co-transfected with pRL-CMV into the cells, and 6 h later, an extract was made and assays performed for firefly and renilla luciferase. A decrease in the ratio of firefly:renilla activity indicates DSB formation. As can be seen from Figure 1A, the two types of non-DSB clusters resulted in lower firefly renilla luciferase activity compared with the undamaged sequence in the WT and ART$^{-/-}$ cells. This indicates the non-DSB clusters were converted to DSBs in these cells. However, there was no significant difference between the WT and ART$^{-/-}$ cells for the same type of non-DSB-clustered lesion. This indicates a similar amount of DSB formation occurred at the non-DSB clusters in the two cell types, and hence the loss of Artemis did not compromise the conversion of the furans to DSBs. Since Apex1 has been implicated in the conversion of these clustered lesions to DSBs (20,25), a protein sample at the time of transfection was also collected for each experiment to determine the Apex1 protein level. No significant difference in protein level was seen between the samples for the different cell lines (data not shown).

Loss of Artemis did not decrease plasmid survival

The introduction of a DSB at a clustered lesion in plasmid DNA can result in destruction of the linear DNA or mis-repaired plasmid. Therefore, examining plasmid survival allows us to determine whether a particular protein, in this case Artemis, is important for DSB repair of the plasmid. The defect in ART$^{-/-}$ cells compromises the repair of DSBs that normally take between 2 and 20 h to repair (33). In our previous studies using this same plasmid system, we examined DNA re-isolated at 2 and 6 h after transfection and found that by 6 h we could detect DNA degradation of plasmid DNA even when there was only a single lesion in the DNA (20). We therefore chose the 2-h time point to study plasmid survival to prevent the results from being altered by plasmid DNA degradation that was not related to the DSB introduced at the clustered lesion.

Three separate ligations of undamaged DNA and each type of clustered lesion were transfected into WT and ART$^{-/-}$ cells.

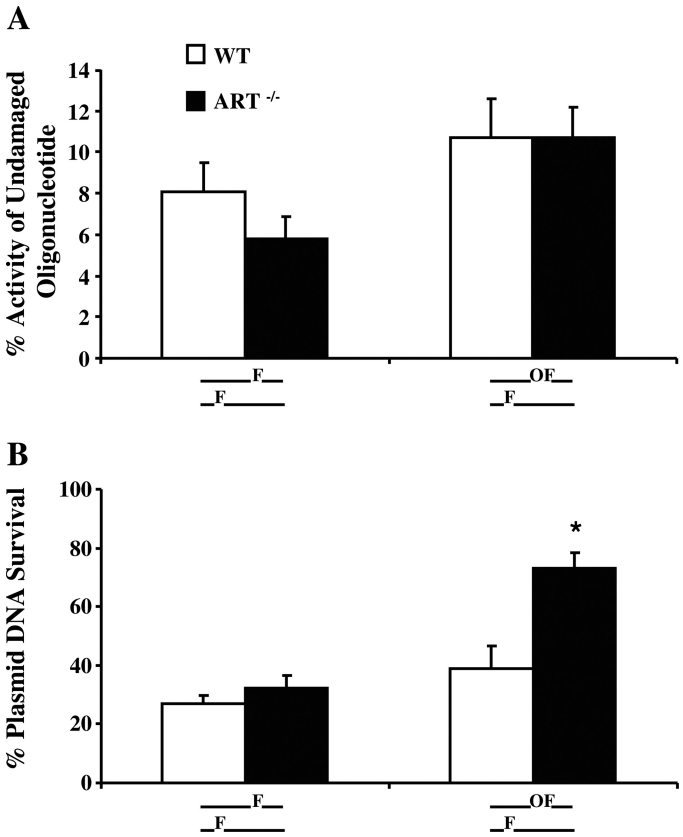

Fig. 1. Loss of Artemis does not alter the cleavage of furans within a clustered lesion or reduce plasmid survival. WT or ART$^{-/-}$ mouse fibroblasts were transfected with ligation reactions containing pCMV3′luc with no damage, or clustered lesions consisting of two closely opposed furans (F) 5 bp apart, or two opposing furans with an 8oxoG (O) situated in tandem 5′ to one of the furans. To determine whether the clustered lesions were converted to DSBs, the ligations were co-transfected with pRL-CMV, and firefly and renilla luciferase activities were measured from a cell-free extract after 6 h (**A**). The firefly/renilla ratio for each construct was expressed as a percentage of the average ratio of the undamaged sequence. At least six transfections of each type of ligation were performed. The average and the standard error are shown graphically in (A). To determine plasmid survival, the ligations were co-transfected with pACYC184, and DNA was re-isolated from the cells after 2 h. Three DNA samples were obtained from three independent ligations and transfections. Each DNA sample was transformed two times into bacteria and the culture grown on solid medium containing carbenicillin or chloramphenicol. A ratio of Carb^R colonies/Cm^R colonies was calculated and plasmid DNA survival calculated by determining the percentage of Carb^R/Cm^R for the clustered lesion divided by the average ratio for the undamaged construct. The average and the standard error are shown graphically in (**B**). Asterisk represents a statistical difference ($P \leq 0.05$) compared with results for the same type of clustered damage from the WT cells.

DNA was re-isolated after 2 h and the percent survival calculated from the number of colonies that were obtained for the re-isolated damaged plasmid and undamaged plasmid after transformation into bacteria. As can be seen from Figure 1B, plasmids that contained two opposing furans (Lesion I, Table I) survived 26–32% compared with the undamaged plasmid, and there was no significant difference between survival in the WT and ART$^{-/-}$ cells. However, the plasmid containing two furans and an 8oxoG (Lesion II) actually survived better in ART$^{-/-}$ cells compared with WT. This was not due to less DSB formation at this lesion in the ART$^{-/-}$ cells, as seen by the luciferase activity expressed from these plasmids in Figure 1A.

Loss of Artemis reduced accuracy of repair

To determine the accuracy of repair, the bacterial colonies carrying the plasmid from the plasmid survival study (Figure 1B) were subjected to PCR analysis. Primers were positioned across the region of the original site of damage in pCMV3′luc. Different pairs of primers situated at increasing distances from the PacI–ClaI region were used to determine the size of the deletions that had been introduced during the repair of the plasmid. A total of 134 colonies were examined for Lesion I from WT cells, while 144 colonies were analysed for the ART$^{-/-}$ cells. For Lesion II, 73 and 142 colonies were analysed for the WT and ART$^{-/-}$ cells, respectively. The sizes of the PCR products were used to determine the deletion sizes. Fisher's exact test was performed to determine whether there was a significant difference in the proportion of colonies containing deletions between the cell types. The DNA that was recovered from the ART$^{-/-}$ cells had a significantly higher percentage of colonies with plasmids containing deletions at the site of the clustered lesion for both Lesions I and II compared with the WT cells (Table II).

To determine whether the deletion size had increased due to a particular lesion and cell type, the results were categorised into groups of deletion size: 0, <100, 100–1000 and >1000 bp. These groups were chosen due to the limits of detection in the change of PCR product size. By the chi-square test, there was a statistically significant alteration in the proportion of colonies distributed among the different deletion size groups for the repair products from plasmids with Lesions I and II for DNA from ART$^{-/-}$ cells compared with the WT cells (Figure 2A and B). Using the Cochran Armitage Trend Test, it was further determined that there was a trend for an increased proportion of colonies to contain plasmid with greater deletion sizes for DNA re-isolated from the ART$^{-/-}$ cells compared with the WT cells. This was found for plasmids containing Lesion I (P = 0.0015) and Lesion II (P = 0.0448). Therefore, the DNA re-isolated from the ART$^{-/-}$ cells tended to contain larger deletions compared with that re-isolated from the WT cells.

It was possible that this increased deletion size in the DNA was not related to the type of DSBs generated from the non-DSB-clustered lesions, but that this was a general defect in ART$^{-/-}$ cells. The experiment was, therefore, repeated using ClaI-linearised pCMV3′luc DNA, which contained DSB termini with 3′ hydroxyl and 5′ phosphate groups that can easily be ligated. The number of colonies analysed by PCR was 51 and 41 for WT and ART$^{-/-}$ cells, respectively. There was no significant difference in the proportion of colonies carrying plasmids with deletions when the WT and ART$^{-/-}$ cells were compared by Fisher's exact test (Table II), and as can be seen from Figure 2C, there was no significant difference in the proportion of colonies within the different deletion size groups. The Cochran Armitage Trend Test also did not detect a trend for the DNA re-isolated from ART$^{-/-}$ cells to contain larger or smaller deletions compared with the WT cells (P = 0.381).

Reducing the level of Mre11 protein did not alter plasmid survival in WT or ART$^{-/-}$ cells

Mre11 is a nuclease that has been implicated in the processing and repair of DSBs by deletional NHEJ (36,37) and has also been implicated in the post-DNA-incision steps of BER in yeast (39). Since the DSBs under examination in this study were generated in the cell by BER (20,25), we postulated that Mre11 may be introducing the deletions at the DSB termini in the absence of Artemis. WT and ART$^{-/-}$ cells were transfected with siRNA to reduce the level of Mre11 protein in the cells. After 24 h, Mre11 expression was reduced by ~75% in WT cells and ~55% in ART$^{-/-}$ cells (Figure 3A). Experiments were performed where the WT and ART$^{-/-}$ cells were first transfected with the siRNA and after 24 h re-transfected with ligations that contained undamaged DNA or DNA with Lesion II. The DNA was re-isolated after 2 h and the experiment was performed three independent times. The plasmid survival was then assessed. There was no significant difference in plasmid survival in the WT or ART$^{-/-}$ cells between the mock-, siControl- or siMre11-transfected cells (Figure 3B). There was also no significant difference in plasmid survival between the WT and ART$^{-/-}$ mock-transfected cells. This is different from the plasmid survival results for the Lesion II-containing plasmids when

Table II. Plasmid DNA containing clustered Lesion I or II contained more deletions following repair in ART$^{-/-}$ cells

Type of DNA substrate	Cell type	Number of colonies (%)	
		No deletion	With deletion
Lesion I (two furans)	WT	32 (24)	102 (76)
	ART$^{-/-}$	12 (8)	132 (92)*
Lesion II (two furans and an 8oxoG)	WT	27 (37)	46 (63)
	ART$^{-/-}$	17 (12)	125 (88)*
Linear DNA	WT	32 (63)	19 (37)
	ART$^{-/-}$	22 (54)	19 (46)

Bacterial colonies from the plasmid survival were subjected to PCR analysis to determine the number of colonies carrying plasmids with deletions. Fisher's exact test using the SAS/STAT Software 9.2 of SAS system for Windows (SAS Institute Inc., Cary, NC, USA) was performed to determine whether there was a significant difference between the number of deletions detected in the DNA re-isolated from WT and ART$^{-/-}$ cells for a particular DNA substrate. A two-sided P value was used to determine whether there was an increase or decrease in the number of colonies with deletions. The colony number was converted to a percentage of the total colonies and this percentage is shown in parentheses.
*P < 0.05 was considered significant.

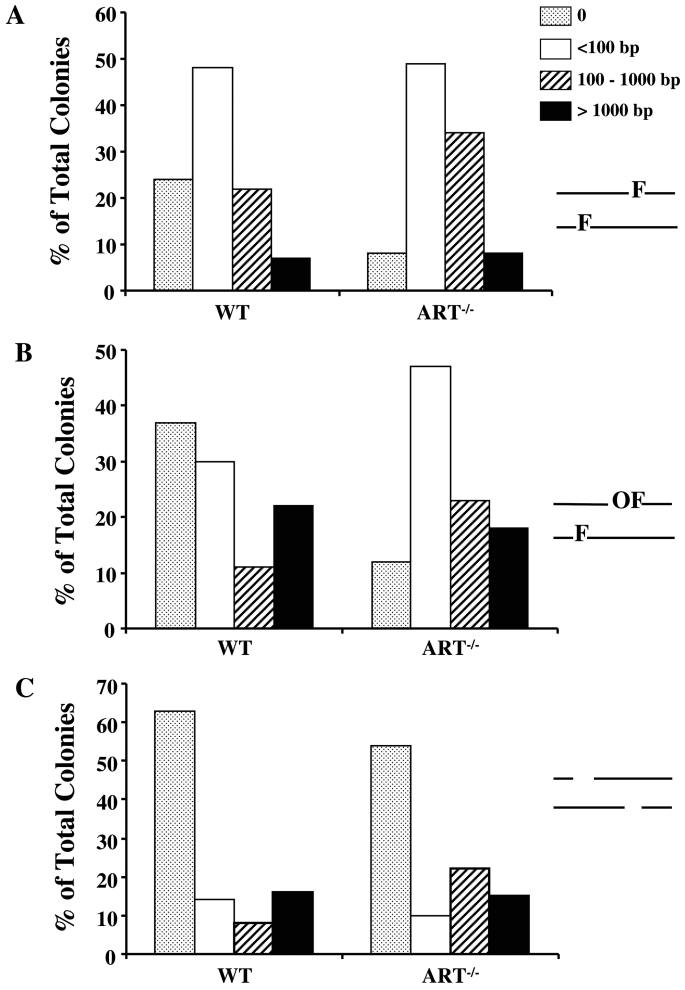

Fig. 2. PCR analysis of colonies obtained from DNA re-isolated from WT and ART$^{-/-}$ cells. Carb^R colonies obtained from the plasmid survival experiments (Figure 1B) were analysed by PCR for deletions in pCMV3′luc. A total of 134 colonies from the three different ligations were examined for Lesion I from WT cells, while 144 colonies were analysed for the ART$^{-/-}$ cells. For Lesion II, 73 and 142 colonies were analysed for the WT and ART$^{-/-}$ cells, respectively. As a control, DNA with a DSB without damaged termini (ClaI-digested pCMV3′luc) was also transfected into WT and ART$^{-/-}$ cells. DNA was re-isolated after 2 h and PCR analysis performed using the Carb^R colonies obtained following transformation of the DNA into bacteria. For the linearised plasmid DNA, 51 and 41 colonies were examined for deletions from the DNA re-isolated from WT and ART$^{-/-}$ cells, respectively. From the PCR analyses, the colonies for each repair substrate were assigned to groups by size of deletion: 0, <100, 100–1000 and >1000 bp. For each repair substrate and cell type, the number of colonies in each group was converted to a percentage of the total analysed colonies. The chi-square statistical test was used to compare the results for WT and ART$^{-/-}$ cells for each substrate. This test determined whether there was a significant change between the cell types in the proportion of colonies that contained the different deletion sizes. These results are shown graphically for Lesion I ($P = 0.0021$) in (**A**), Lesion II ($P < 0.0001$) in (**B**) and for ClaI-linearised DNA ($P = 0.2796$) in (**C**).

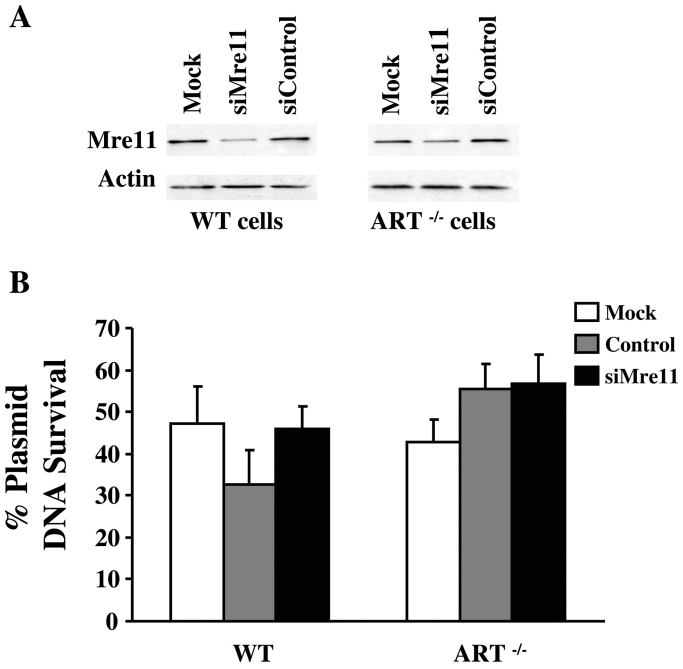

Fig. 3. Decreasing Mre11 in WT or ART$^{-/-}$ cells does not alter plasmid survival. Cells were transfected with siRNA designed against Mre11, a scrambled control siRNA (siControl) or no siRNA (mock) and incubated for 24 h. A cell-free extract was prepared from some of the cell population and analysed by western analysis for Mre11 expression (**A**). The remaining cells were transfected with pACYC184 and pCMV3′luc ligations containing no damage or Lesion II (two furans and an 8oxoG). DNA was re-isolated after 2 h. Three DNA samples were obtained from three independent ligations and transfections. Each DNA sample was transformed two times into bacteria and the culture grown on solid medium containing carbenicillin or chloramphenicol. A ratio of Carb^R colonies/Cm^R colonies was calculated, and plasmid DNA survival calculated by determining the percentage of Carb^R/Cm^R for the clustered lesion divided by the average ratio for the undamaged construct. The average and the standard error are shown graphically in (**B**).

the cells were transfected only once (Figure 1B). Interestingly, there was an increase in survival of plasmids with Lesion II in the ART$^{-/-}$ siControl-transfected samples compared with the WT siControl samples, although this was not quite significant by a *t*-test ($P = 0.0584$). It is, therefore, possible that the loss of Artemis in the cells may alter plasmid survival for Lesion II-containing plasmids. Further work that is beyond the scope of this study is required to determine the reason for this potential increase in survival.

Reducing the level of Mre11 protein did not alter the deletion sizes of the repaired plasmid

The colonies obtained from the plasmid survival experiment (Figure 3B) were analysed by PCR to determine the size of deletions introduced during the repair of DSBs produced from Lesion II. We analysed the colonies from the WT mock transfection and ART$^{-/-}$ siControl transfection as the control samples, since the colonies for the second control group in each cell type were lost during the colony processing. However, these control WT and ART$^{-/-}$ samples were appropriate control samples since they showed no significant trend of an increase/decrease in deletion size compared with the data obtained for the first set of WT and ART$^{-/-}$ samples, respectively. Reducing Mre11 in the WT cells did result in a slight increase in the percentage of colonies carrying deletions ($P = 0.0457$, Fisher's exact test): 85% of colonies carried deletions from the siMre11-transfected cells compared with 75% in the case of the mock-transfected cells. However, there was no significant increase in the percentage of colonies with deletions when the ART$^{-/-}$ siControl samples (83% carried deletions) and ART$^{-/-}$ siMre11 samples (86% carried deletions) were compared. When the PCR results were used to categorise the deletions into different size groups (0, <100, 100–1000 and >1000 bp), there was no significant difference in the distribution of the colonies among the different deletion size groups (chi-square test) between the WT mock-transfected and the WT siMre11-transfected cells

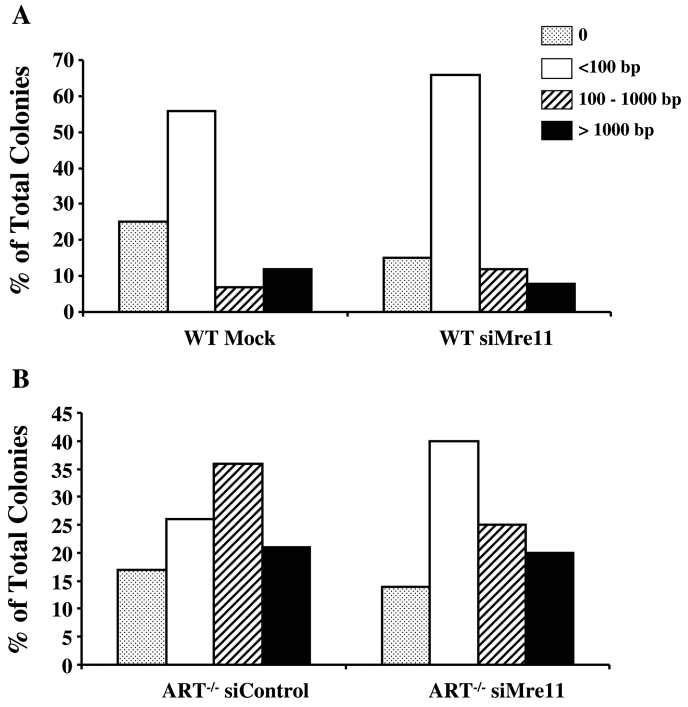

Fig. 4. PCR analysis of colonies obtained from DNA re-isolated from WT and ART$^{-/-}$ cells after knock-down of Mre11 by siRNA. Carb^{R} colonies obtained from the plasmid survival experiments following the treatment of WT or ART$^{-/-}$ cells with siMre11 (Figure 3B) were analysed by PCR for deletions in pCMV3′luc. Colonies from the mock-transfected (no siRNA treatment) or the siControl-transfected cells were analysed for comparison. Twenty-six to 51 colonies were analysed per independent DNA sample re-isolated from the cells. Hence, a total of 102 and 129 colonies were examined for the presence of deletions in the plasmid for Lesion II (two furans and an 8oxoG) for WT mock- and siMre11-transfected cells, respectively, while 112 and 119 colonies were studied for siControl- and siMre11-transfected ART$^{-/-}$ cells, respectively. From the PCR analyses, the colonies for each test condition were assigned to groups by size of deletion: 0, <100, 100–1000 and >1000 bp. For each test condition, the number of colonies in each group was converted to a percentage of the total analysed colonies. The chi-square test was used to compare the results for WT and ART$^{-/-}$ cells for each substrate. This test determined whether there was a significant change between the transfected cell types in the proportion of colonies that contained the different deletion sizes. These results are shown graphically for mock- and siMre11-transfected WT cells ($P = 0.0845$) in (**A**) and for siControl- and siMre11-transfected ART$^{-/-}$ cells ($P = 0.1106$) in (**B**).

(Figure 4A), and between the ART$^{-/-}$ siControl-transfected and the ART$^{-/-}$ siMre11-transfected cells (Figure 4B). The Cochran Armitage Trend Test also did not detect a trend for a change in the deletion size for the DNA re-isolated from the WT mock-transfected and WT siMre11-transfected cells ($P = 0.4868$) and between the ART$^{-/-}$ siControl-transfected and the ART$^{-/-}$ siMre11-transfected cells ($P = 0.4257$). Reducing Mre11 in the two cell types, therefore, had no effect on the size of deletions in the repair products.

Discussion

Both high and low LET radiation produce non-DSB-clustered lesions, DSBs and complex DSBs in DNA (42), and the non-DSB-clustered lesions have been detected following irradiation of cells at doses commonly used for radiotherapy (42,43). High LET radiation has a higher relative biological effectiveness (RBE) for cell killing than low LET radiation, and one explanation of this increase in RBE could be the increase in the complexity of the damage and the inability of the cell to repair the complex damage. The predominant form of radiation used in the clinic for cancer treatment is low LET X-rays or gamma rays. However, there are 40 particle radiation therapy centres in the world and a number of these treat patients with high LET carbon ions. By March 2012, 96,537 patients had been treated with particle radiation therapy, and there are 25 new centres that plan to open before 2016 (44). To improve radiotherapy or to design complementary treatments that enhance the efficacy of high and low LET radiotherapy, it is necessary to understand how tumour cells try to repair the non-DSB-clustered lesions and the resulting DSBs or complex DSBs produced by repair of non-DSB-clustered damage. It was originally hypothesised that the defect in ART$^{-/-}$ cells was the repair of complex DSBs (33), and Artemis has been shown to be involved in the repair of DSBs with an AP site situated near the break (28). More recent studies implicate Artemis in the repair of DSBs in heterochromatin (34,35), and so this work was performed to determine whether Artemis plays a role in processing complex DSB termini generated from the initiation of BER at defined non-DSB-clustered lesions in cells.

The clustered lesions examined (Lesions I and II, Table I) each contained two opposing furans, and Lesion II also had an 8oxoG situated 5′ to one of the furans. These lesions have been well characterised in our previous studies (20,25): Lesions I and II are converted to DSBs by the major class II AP endonuclease in the cell (Apex1 in mouse cells) and NHEJ is involved in the repair of these DSBs. The DSB introduced at Lesion II is likely to be a complex DSB since it was clearly demonstrated that Apex1 in a nuclear extract cleaves at the furans in Lesion II prior to removal of the 8oxoG by Ogg1 (20). The only other possible scenario where 8oxoG could be removed prior to DSB formation is if the furan on the non-transcribed strand (Table I) was removed first to generate a 3′ terminal 8oxoG near a SSB. This terminal 8oxoG is still difficult to repair as it is not a substrate for the DNA glycosylases Neil1, Neil2 or Ogg1 (45). There is *in vitro* evidence showing that human Ape1, and hence Apex1 in mouse cells, has limited ability to remove a 3′ terminal 8oxoG at a SSB: 600 fmol of Ape1 was required to remove only ~50% of the 8oxoG in 250 fmol of substrate in 20 min at 37°C (45). However, in cells, it is unlikely that a 3′ terminal 8oxoG at a SSB would be generated at Lesion II as the 8oxoG situated 5′ and in tandem to the furan reduces the activity of Apex1 at the furan (20). The order of damage removal would likely be the furan from the transcribed strand, followed by the furan from the non-transcribed strand. Therefore, according to substrate specificity, Apex1 in cells will convert Lesion II to a complex DSB with 8oxoG situated on a 3′ overhang at one of the 3′ termini of the DSB.

Whenever Apex1 cleaves at a furan, the SSB that is generated has a 5′-blocked terminus due to the structure of the furan lesion, and 8oxoG situated near a DSB has been found to reduce the efficiency of ligation of the DNA termini (45,46). Therefore, the DSB termini generated from Lesions I and II by Apex1 in mouse cells need to be processed by other enzymes to remove the 5′-blocked termini and to remove the 8oxoG from the complex DSB prior to repair. These substrates were, therefore, appropriate to test the involvement of Artemis in the repair of complex DSBs generated from non-DSB clusters.

Lesions I and II were efficiently converted to DSBs in WT and ART$^{-/-}$ cells, and there was no reduction in plasmid survival. A consistent difference that was found between the WT and ART$^{-/-}$ cells was an increase in the size of deletions detected in

the repair products from the DNA re-isolated from ART$^{-/-}$ cells. This increase in deletion size was not related to the presence of 8oxoG, and hence the complexity of the DSB, as a similar trend for deletion size was found for Lesions I and II. This was also not a general ART$^{-/-}$ cell DSB repair defect as there was no difference in the repair products from WT and ART$^{-/-}$ cells for linear plasmids with 3′-hydroxyl and 5′-phosphate termini. The barrier to repair that is absent from restriction-digested linear DNA but common to the DSBs generated from Lesions I and II is the 5′-blocked termini created by Apex1 at the furans. This study, therefore, implicates Artemis not necessarily in the repair of complex DSBs but in the processing of DSBs with 5′-blocked termini. This is in agreement with previous studies that linked the Artemis endonuclease to the sensitivity of cells to damaging agents generating 5′- and 3′-blocked termini (32). Therefore, our study suggests Artemis will also be required for NHEJ to process DSBs generated from ionising radiation-induced non-DSB-clustered lesions containing oxidised AP sites and/or SSBs with a nucleoside 5′ aldehyde (7). Oxidised AP sites are substrates for human Ape1 and so opposing oxidised AP sites would result in DSBs with 5′-blocked termini.

Previous studies examining situations that inhibit/reduce NHEJ have found increased end resection at the DSB (47,48). In fact, reducing expression of DNA-PKcs using siRNA increased the resection at DSBs (48). This is relevant to Artemis, as DNA-PK is required to activate the Artemis endonuclease (29). In NHEJ protein-deficient cells, homologous recombination is increased (49), and cells with reduced DNA-PKcs and Ku80 have an increase in RPA foci after X-rays, which indicates an increase in end resection (48). These published studies, therefore, suggest that the increase in the size of deletions detected in repair products in our work was due to the impairment of NHEJ when Artemis was not available to remove the 5′-blocked termini. If repair cannot occur by the classical NHEJ pathway, then either homologous recombination or the alternative backup NHEJ pathway can be used [for review, see ref. (38)], and an increase in end resection is an indicator of repair by these pathways. We detected Ku-independent repair of the DSB generated from Lesion I in our previous study in Ku-deficient cells (25).

Mre11 forms a complex with Rad50 and Nbs1 (MRN) and is known to be involved in end resection during homologous recombination [for review, see ref. (38)]. More recently, the Mre11 nuclease activity has been implicated in the alternative NHEJ pathway. The alternative NHEJ pathway does not require the Ku70/80 complex, but involves the MRN complex binding the ends of the DNA. MRN in combination with CtIP resects the DNA, pausing when microhomology sequences are found at the two termini (50–52). Ligation occurs at the microhomology sequences to complete DSB repair [for review, see refs (38,53)]. This alternative NHEJ pathway is characterised by large deletions, and reducing Mre11 protein expression in human cells has been found to substantially decrease alternative NHEJ repair but not alter classical NHEJ (54). In *Schizosaccharomyces pombe*, the Mre11 nuclease is important for initiation of end resection as it is needed to remove the Ku70/80 complex and the MRN complex from DSBs (55). Since in our situation classical NHEJ was likely impaired by the inability to remove 5′-blocked termini in the absence of Artemis, we postulated that Mre11 might be required to remove the Ku heterodimer to allow access to the DSB and/or be involved in end resection to generate the deletions by either alternative NHEJ or homologous recombination. However, when Mre11 protein expression was reduced to below 50% the normal level in WT and ART$^{-/-}$ cells, there was no alteration in the deletion sizes detected in the repair products. It is possible that Mre11 needed to be reduced to an even lower expression level to see an effect on deletion size. However, in support of the conclusion that Mre11 is not the nuclease promoting end resection in the absence of Artemis in this study, DNA degradation by Mre11 has been found to be inhibited by cohesive ends and stimulated by mismatched DNA ends (56). The DSB created by Apex1 at the opposing furans has overhangs with sequence homology and so should not be a good substrate for Mre11. It is possible, therefore, that other nucleases introduce the deletions at the DSBs generated from Lesions I and II when Artemis is absent. Two potential candidates are CtIP and ExoI (57), both of which are involved in DNA end resection in homologous recombination (38). CtIP has also been implicated in end processing during alternative NHEJ (52).

In summary, this study implicates Artemis in the processing of the 5′-blocked termini at simple or complex DSBs that can be generated from non-DSB-clustered lesions during radiotherapy. The lack of Artemis did not compromise the amount of repair, but altered the size of the deletion introduced at the break site during DSB repair. The presence of oxidative DNA damage at the DSB did not influence the type of repair product in ART$^{-/-}$ cells. The 5′-blocked termini and not the added 8oxoG influenced the need for processing by Artemis. It is possible that the lack of ability to process the 5′ termini of the DSB impaired classical NHEJ enough to result in a change in the type of DSB repair. A requirement for Artemis to remove the 8oxoG at the DSB would then have been masked by the dominating effect of the 5′-blocked termini generated by Apex1 at the furans. The increase in deletion size in the absence of Artemis suggests that repair switched to the alternative NHEJ repair pathway or single-strand annealing. It is unlikely that homologous recombination completed repair due to the inaccuracy of repair. Future studies are needed to determine which nuclease/nucleases are involved in processing the blocked termini in the absence of Artemis.

This work indicates that inhibition of Artemis alone at the time of radiotherapy would not improve therapeutic outcome. The inhibition of one repair pathway seems to promote the use of an alternative mechanism to complete repair of DSBs generated by the radiation or from the initiation of BER at a non-DSB-clustered lesion. In fact, promoting mutagenic repair could result in tumour recurrence. This work needs to be extended in the future to reveal which proteins are involved in processing complex DSBs or DSBs with blocked termini during NHEJ and the backup repair pathways. Since high LET therapies are now being used to treat cancer, it is even more important to dissect the repair mechanisms of these clustered lesions and complex DSBs. Understanding the processing and outcome of these lesions could lead to therapeutic strategies that manipulate the tumour cell's DNA repair capacity and to the design of complementary treatments that enhance the efficacy of radiotherapy.

Funding

This work was supported by the National Cancer Institute at the National Institutes of Health (CA85693 and CA85693-09S1).

Conflict of interest statement: None declared.

References

1. Munro, T. R. (1970) The relative radiosensitivity of the nucleus and cytoplasm of Chinese hamster fibroblasts. *Radiat. Res.*, **42**, 451–470.
2. Limoli, C. L., Corcoran, J. J., Milligan, J. R., Ward, J. F. and Morgan, W. F. (1999) Critical target and dose and dose-rate for the chromosomal instability by ionizing radiation. *Radiat. Res.*, **151**, 677–685.
3. Teoule, R. (1987) Radiation induced DNA damage and its repair. *Int. J. Radiat. Biol.*, **51**, 573–589.
4. Oleinick, N. L., Chiu, S. M., Ramakrishnan, N. and Xue, L.-Y. (1987) The formation, identification, and significance of DNA-protein cross-links in mammalian cells. *Br. J. Cancer*, **55**(Suppl. VIII), 135–140.
5. Henner, W. D., Rodriguez, L. O., Hecht, S. M. and Haseltine, W. A. (1983) γ ray induced deoxyribonucleic acid strand breaks. *J. Biol. Chem.*, **258**, 711–713.
6. Ward, J. F. (1988) DNA damage produced by ionizing radiation in mammalian cells: identities, mechanisms of formation, and reparability. *Prog. Nucleic Acid Res. Mol. Biol.*, **35**, 95–125.
7. Chan, W., Chen, B., Wang, L., Taghizadeh, K., Demott, M. S. and Dedon, P. C. (2010) Quantification of the 2-deoxyribonolactone and nucleoside 5′-aldehyde products of 2-deoxyribose oxidation in DNA and cells by isotope-dilution gas chromatography mass spectrometry: differential effects of gamma-radiation and Fe2+-EDTA. *J. Am. Chem. Soc.*, **132**, 6145–6153.
8. Sung, J. S., DeMott, M. S. and Demple, B. (2005) Long-patch base excision DNA repair of 2-deoxyribonolactone prevents the formation of DNA-protein cross-links with DNA polymerase beta. *J. Biol. Chem.*, **280**, 39095–39103.
9. Jacobs, A. C., Kreller, C. R. and Greenberg, M. M. (2011) Long patch base excision repair compensates for DNA polymerase β inactivation by the C4′-oxidized abasic site. *Biochemistry*, **50**, 136–143.
10. Ward, J. F. (1987) Radiation and hydrogen peroxide induced free radical damage to DNA. *Br. J. Cancer*, **55**(Suppl. VIII), 105–112.
11. Sutherland, B. M., Bennett, P. V., Sutherland, J. C. and Laval, J. (2002) Clustered DNA damages induced by X-rays in human cells. *Radiat. Res.*, **157**, 611–616.
12. Ward, J. F. (1995) Radiation mutagenesis: the initial DNA lesions responsible. *Radiat. Res.*, **142**, 362–368.
13. Prise, K. M., Ahnstrom, G., Belli, M. *et al.* (1998) A review of dsb induction data for varying quality radiations. *Int. J. Radiat. Biol.*, **74**, 173–184.
14. Semenenko, V. A. and Stewart, R. D. (2006) Monte Carlo simulation of DNA damage formed by electrons and light ions. *Phys. Med. Biol.*, **51**, 1693–1706.
15. Sage, E. and Harrison, L. (2011) Clustered DNA lesion repair in eukaryotes: relevance to mutagenesis and survival. *Mutat. Res.*, **711**, 123–133.
16. Nikjoo, H., O'Neill, P., Wilson, W. E. and Goodhead, D. T. (2001) Computational approach for determining the spectrum of DNA damage induced by ionizing radiation. *Radiat. Res.*, **156**, 577–583.
17. Wallace, S. S., Murphy, D. L. and Sweasy, J. B. (2012) Base excision repair and cancer. *Cancer Lett.*, **327**, 73–89.
18. Harrison, L. (2013) Radiation induced DNA damage, repair and therapeutics. In: Madhusudan, S. and Wilson, D. M., III (eds), *DNA Repair and Cancer. Chapter 4*. Science Publishers/CRC Press, Boca Raton, FL, pp. 92–136.
19. Malyarchuk, S., Brame, K. L., Youngblood, R., Shi, R. and Harrison, L. (2004) Two clustered 8-oxo-7,8-dihydroguanine (8-oxodG) lesions increase the point mutation frequency of 8-oxodG, but do not result in double strand breaks or deletions in *Escherichia coli*. *Nucleic Acids Res.*, **32**, 5721–5731.
20. Malyarchuk, S., Castore, R. and Harrison, L. (2009) Apex1 can cleave complex clustered lesions in cells. *DNA Repair*, **8**, 1343–1354.
21. Malyarchuk, S., Youngblood, R., Landry, A. M., Quillin, E. and Harrison, L. (2003) The mutation frequency of 8-oxo-7,8-dihydroguanine (8-oxodG) situated in a multiply damaged site: comparison of a single and two closely opposed 8-oxodG in *Escherichia coli*. *DNA Repair*, **2**, 695–705.
22. Yang, N., Galick, H. and Wallace, S. S. (2004) Attempted base excision repair of ionizing radiation damage in human lymphoblastoid cells produces lethal and mutagenic double strand breaks. *DNA Repair*, **3**, 1323–1334.
23. D'souza, D. and Harrison, L. (2003) Repair of clustered uracil DNA damages in *Escherichia coli*. *Nucleic Acids Res.*, **31**, 4573–4581.
24. Harrison, L., Brame, K. L., Geltz, L. E. and Landry, A. M. (2006) Closely opposed apurinic/apyrimidinic sites are converted to double strand breaks in *Escherichia coli* even in the absence of exonuclease III, endonuclease IV, nucleotide excision repair and AP lyase cleavage. *DNA Repair*, **5**, 324–335.
25. Malyarchuk, S., Castore, R. and Harrison, L. (2008) DNA repair of clustered lesions in mammalian cells: involvement of non-homologous end-joining. *Nucleic Acids Res.*, **36**, 4872–4882.
26. Kozmin, S., Sedletska, Y., Reynaud-Angelin, A., Gasparutto, D. and Sage, E. (2009) The formation of double strand breaks at multiply damaged sites is driven by the kinetics of excision/incision at base damage in eukaryotic cells. *Nucleic Acids Res.*, **37**, 1767–1777.
27. Kasparek, T. R. and Humphrey, T. C. (2011) Double-strand break repair pathways, chromosomal rearrangements and cancer. *Semin. Cell Dev. Biol.*, **22**, 886–897.
28. Covo, S., de Villartay, J.-P., Jeggo, P. A. and Livneh, Z. (2009) Translesion DNA synthesis-assisted non-homologous end-joining of complex double-strand breaks prevents loss of DNA sequences in mammalian cells. *Nucleic Acids Res.*, **37**, 6737–6745.
29. Ma, Y., Pannicke, U., Schwarz, K. and Lieber, M. R. (2002) Hairpin opening and overhang processing by an Artemis/DNA-dependent protein kinase complex in nonhomologous end joining and V(D)J recombination. *Cell*, **108**, 781–794.
30. Goodarzi, A. A., Yu, Y., Riballo, E. *et al.* (2006) DNA-PK autophosphorylation facilitates Artemis endonuclease activity. *EMBO J.*, **25**, 3880–3889.
31. Povirk, L. F., Zhou, T., Zhou, R., Cowan, M. J. and Yannone, S. M. (2007) Processing of 3′-phosphoglycolate-terminated DNA double strand breaks by Artemis nuclease. *J. Biol. Chem.*, **282**, 3547–3558.
32. Mohapatra, S., Kawahara, M., Khan, I. S., Yannone, S. M. and Povirk, L. F. (2011) Restoration of G1 chemo/radioresistance and double-strand break repair proficiency by wild-type but not endonuclease-deficient Artemis. *Nucleic Acids Res.*, **39**, 6500–6510.
33. Riballo, E., Kuhne, M., Rief, N. *et al.* (2004) A pathway of double strand break repair rejoining dependent upon ATM, Artemis, and proteins locating to gamma-H2AX foci. *Mol. Cell*, **16**, 715–724.
34. Goodarzi, A. A., Noon, A. T., Deckbar, D., Ziv, Y., Shiloh, Y., Lobrich, M. and Jeggo, P. A. (2008) ATM signaling facilitates repair of DNA double-strand breaks associated with heterochromatin. *Mol. Cell*, **31**, 167–177.
35. Woodbine, L., Brunton, H., Goodarzi, A. A., Shibata, A. and Jeggo, P. A. (2011) Endogenously induced DNA double strand breaks arise in heterochromatic DNA regions and require ataxia telangiectasia mutated and Artemis for their repair. *Nucleic Acids Res.*, **39**, 6986–6997.
36. Zhuang, J., Jiang, G., Willers, H. and Xia, F. (2009) Exonuclease function of human Mre11 promotes deletional nonhomologous end joining. *J. Biol. Chem.*, **284**, 30565–30573.
37. Rass, E., Grabarz, A., Plo, I., Gautier, J., Bertrand, P. and Lopez, B. S. (2009) Role of Mre11 in chromosomal nonhomologous end joining in mammalian cells. *Nat. Struct. Mol. Biol.*, **16**, 819–824.
38. Stracker, T. H. and Petrini, J. H. J. (2011) The MRE11 complex: starting from the ends. *Nat. Rev. Mol. Cell Biol.*, **12**, 90–103.
39. Steininger, S., Ahne, F., Winkler, K., Kleinschmidt, A., Eckardt-Schupp, F. and Moertl, S. (2010) A novel function for the Mre11-Rad50-Xrs2 complex in base excision repair. *Nucleic Acids Res.*, **38**, 1853–1865.
40. Malyarchuk, S. and Harrison, L. (2005) DNA repair of clustered uracils in HeLa cells. *J. Mol. Biol.*, **345**, 731–743.
41. Rooney, S., Sekiguchi, J., Zhu, C. *et al.* (2002) Leaky scid phenotype associated with defective V(D)J coding end processing in Artemis-deficient mice. *Mol. Cell*, **10**, 1379–1390.
42. Asaithamby, A., Hu, B. and Chen, D. J. (2011) Unrepaired clustered DNA lesions induce chromosome breakage in human cells. *Proc. Natl Acad. Sci. U.S.A.*, **108**, 8293–8298.
43. Sutherland, B. M., Bennett, P. V., Sidorkina, O. and Laval, J. (2000) Clustered DNA damages induced in isolated DNA and in human cells by low doses of ionizing radiation. *Proc. Natl Acad. Sci. U.S.A.*, **97**, 103–108.
44. Jermann, M. (2012). Hadron Therapy Patient Statistics, Particle Therapy Co-Operative Group (PTCOG). http://ptcog.web.psi.ch/ptcentres.html (accessed 16 October, 2012).
45. Parsons, J. L., Dianova, I. I. and Dianov, G. L. (2005) APE1-dependent repair of DNA single-strand breaks containing 3′-end 8-oxoguanine. *Nucleic Acids Res.*, **33**, 2204–2209.
46. Dobbs, T. A., Palmer, P., Maniou, Z., Lomax, M. E. and O'Neill, P. (2008) Interplay of two major repair pathways in the processing of complex double-strand DNA breaks. *DNA Repair*, **7**, 1372–1383.
47. Cui, X., Yu, Y., Gupta, S., Cho, Y.-M., Lees-Miller, S. P. and Meek, K. (2005) Autophosphorylation of DNA-dependent protein kinase regulates DNA end processing and may also alter double-strand break repair choice. *Mol. Cell. Biol.*, **25**, 10842–10852.
48. Shibata, A., Conrad, S., Birraux, J. *et al.* (2011) Factors determining DNA double-strand break repair pathway choice in G2 phase. *EMBO J.*, **30**, 1079–1092.
49. Pierce, A. J., Hu, P., Han, M., Ellis, N. and Jasin, M. (2001) Ku DNA end-binding protein modulates homologous repair of double-strand breaks in mammalian cells. *Genes Dev.*, **15**, 3237–3242.

50. Bennardo, N., Cheng, A., Huang, N. and Stark, J. M. (2008) Alternative-NHEJ is a mechanistically distinct pathway of mammalian chromosome break repair. *PLoS Genet.*, **4**, e1000110.
51. Dinkelmann, M., Spehalski, E., Stoneham, T., Buis, J., Wu, Y., Sekiguchi, J. M. and Ferguson, D. O. (2009) Multiple functions of MRN in end-joining pathways during isotype class switching. *Nat. Struct. Mol. Biol.*, **16**, 808–813.
52. Zhang, Y. and Jasin, M. (2011) An essential role for CtIP in chromosomal translocation formation through an alternative end-joining pathway. *Nat. Struct. Mol. Biol.*, **18**, 80–84.
53. Zha, S., Boboila, C. and Alt, F. W. (2009) Mre11: roles in DNA repair beyond homologous recombination. *Nat. Struct. Mol. Biol.*, **16**, 798–800.
54. Zhuang, J., Jiang, G., Willers, H. and Xia, F. (2009) Exonuclease function of human Mre11 promotes deletional nonhomologous end joining. *J. Biol. Chem.*, **284**, 30565–30573.
55. Langerak, P., Mejia-Ramirez, E., Limbo, O. and Russell, P. (2011) Release of Ku and MRN from DNA ends by Mre11 nuclease activity and Ctp1 is required for homologous recombination repair of double strand breaks. *PLoS Genet.*, **7**, e1002271.
56. Paull, T. T. and Gellert, M. (2000) A mechanistic basis for Mre11-directed DNA joining at microhomologies. *Proc. Natl Acad. Sci. U.S.A.*, **97**, 6409–6414.
57. Tomimatsu, N., Mukherjee, B., Deland, K., Kurimasa, A., Bolderson, E., Khanna, K. K. and Burma, S. (2012) Exo1 plays a major role in DNA end resection in humans and influences double-strand break repair and damage signaling decisions. *DNA Repair*, **11**, 441–448.